

## Raman scattering in large single indium nitride dots: Correlation between morphology and strain

F. Demangeot, J. Frandon, C. Pinquier, and M. Caumont

*Laboratoire de Physique des Solides IRSAMC, UMR 5477 CNRS, 118 Route de Narbonne, Université Paul Sabatier, 31062 Toulouse Cédex 04, France*

O. Briot, B. Maleyre, S. Clur-Ruffenach, and B. Gil

*Groupe d'Etudes des Semiconducteurs, UMR 5650 CNRS, Place Eugène Bataillon, Université Montpellier II, 34095 Montpellier, France*

(Received 31 July 2003; published 11 December 2003)

We present an experimental work on the Raman analysis of single InN dots grown by metal-organic vapor phase epitaxy on GaN buffer layer. InN islands of controlled sizes have been fabricated by taking advantage of the Stranski-Krastanov growth mode. Atomic force microscopy and micro-Raman spectroscopy have been employed to investigate their morphology and internal strain. The usual shape of the dots corresponds to truncated pyramids with a hexagonal base as revealed by atomic force microscopy measurements. The  $E_2$  phonon frequency, detected in micro-Raman spectra recorded from single dots of sizes ranging from 480 nm down to 30 nm in height, allows a rough evaluation of the residual strain field. Careful analysis of these data reveals that the islands are weakly strained, which is likely due to the formation of dislocations near the InN/GaN interface. Nevertheless, the reduction of the size of InN islands leads to an increasing strain field. Finally, we observed a surprisingly small strain increase when the dots are capped with a thin GaN top surface layer. This demonstrates the major role played by the plastic strain relaxation.

DOI: 10.1103/PhysRevB.68.245308

PACS number(s): 73.21.La, 78.30.Fs, 81.15.Gh

Some Raman studies of GaN quantum dots (QD's) have been published in recent years: in particular, the mean strain in stackings of GaN QD's embedded in AlN spacers<sup>1</sup> and the internal deformation in individual GaN islands deposited on AlN have been evaluated.<sup>2</sup> In this paper, we report on an investigation of single InN dots by inelastic light scattering. Not only has their deformation been estimated, but also heterogeneities in the strain field across the dot have been evidenced. InN has recently been the focus of intensive work, especially with regard to a reevaluation of its electronic band-gap energy.<sup>3-7</sup> Currently, an accepted value of this energy would be around 0.7 eV, which opens the way to potential applications for infrared emission and detection. The successful growth of low-density InN quantum dots would permit us to design a single-photon emitter, similar to those recently reported in the InAs/GaAs system.<sup>8</sup> Nevertheless, many questions need to be investigated, such as the emission energy and its efficiency in such structures as a function of the growth parameters. It has been demonstrated that InN quantum dots can be fabricated by using the three-dimensional Stranski-Krastanov growth mode (formation of dislocated islands on the surface).<sup>9,10</sup> The latter takes place after a transition from a two-dimensional (2D) growth mode as a result of strain relaxation in the film, promoted by the large lattice mismatch ( $\sim 11\%$ ) between InN and the GaN template. InN nanostructures and nanowires have also been grown by different growth techniques.<sup>11,12</sup> But an open question still remains: could we expect applications in optoelectronics from those nanoobjects in spite of the observed plastic strain relaxation? Moreover, data concerning electronic properties are still scarce, and such fundamental properties as electron-phonon interaction should be addressed in InN quantum dots, since it is well known that electrons and phonons are strongly coupled in low dimensional semicon-

ductor structures. To date, papers have been published about the phonon physics in InN continuous films grown by different techniques such as metal-organic vapor phase epitaxy (MOVPE),<sup>13-15</sup> molecular-beam epitaxy (MBE),<sup>16-21</sup> atomic layer epitaxy (ALE),<sup>22</sup> reactive sputtering,<sup>23</sup> and by saturating indium metal with atomic nitrogen from a microwave plasma source.<sup>24</sup> Both experimental studies and calculations have furnished data concerning the zone-center phonon frequencies,<sup>13-15,17,19,22-24</sup> the  $\mathbf{q}$  dispersion curves in the first Brillouin zone,<sup>16,18,25</sup> and also the phonon-plasmon coupling.<sup>20</sup> One finds a significant scattering of measured values of InN phonon frequencies which is likely due to varying strain states in the investigated samples. All the phonon frequencies found in the literature can be correlated to the strain state of InN and are consistent with each other. Here, we will concentrate on the study of strain and morphology of InN islands grown on the surface of a GaN layer deposited on sapphire (0001).

Samples were grown by MOVPE. A 1- $\mu\text{m}$  GaN buffer layer was deposited onto a sapphire substrate and then the growth of InN took place, using TMIIn and  $\text{NH}_3$  as precursors. Only one plane of InN islands was grown at the surface. The fabrication parameters investigated during this study were growth temperature ( $T_g$ ) in the range 500–700 °C, V/III molar ratio in the range 7000–30 000, and growth time from 3600 s down to 10 s. It has been found that the nanostructures are rather flat and their density is quite low ( $10^7 \text{ cm}^{-2}$ ). This has been correlated to a high surface diffusion at the growth temperature. It was shown that the diameter of the dots increases with  $T_g$  while the density decreases. Moreover, dot size can be reduced by using higher values of the V/III molar ratio. A detailed analysis of these growth results can be found elsewhere.<sup>10</sup> For large InN dots, the material quality assessment was achieved by x-ray dif-

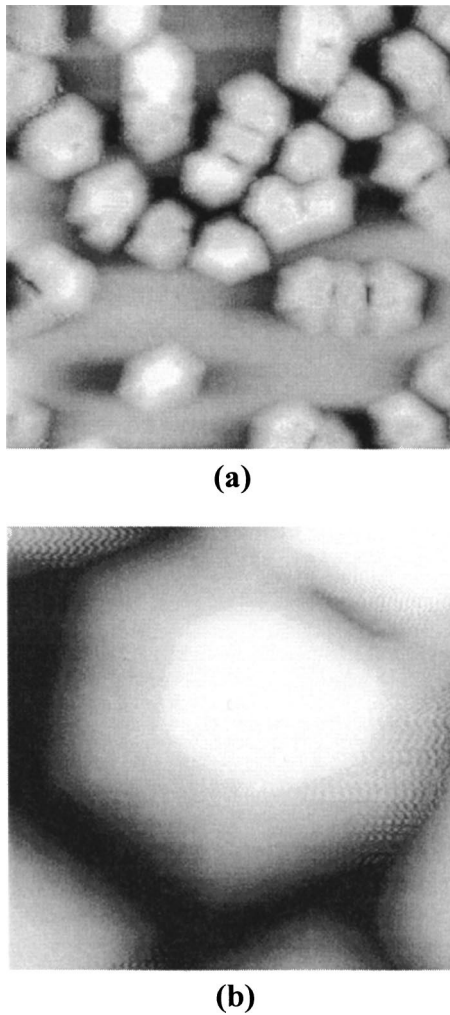


FIG. 1. AFM images of the sample surface containing InN islands. (a) Scan size is  $5 \times 5 \mu\text{m}$ . The average height and average diameter of these dots are, respectively, 180 and 500 nm. (b) AFM image of a single dot. Scan size is  $1 \times 1 \mu\text{m}$ .

fraction, which yielded a full width at half maximum below 400 arcseconds, comparable with its value for the GaN buffer layer and indicative of the high crystalline quality. InN islands of size ranging from 30 nm up to 480 nm in height were characterized by using atomic force microscopy (AFM) and micro-Raman spectroscopy. A Park Scientific Instruments microscope (CP model) was used in the AFM configuration in noncontact mode. Raman experiments were performed with a Renishaw spectrometer equipped with an XYZ automated stage, rejection dielectric filters, and a CCD camera. Micro-Raman spectra were excited using a 514.5-nm (2.41-eV) line of an  $\text{Ar}^+$  laser at low power, and the light was focused through a  $100\times$  magnification objective giving a spot area of  $1 \mu\text{m}$ , which is smaller than the larger dots ( $2.4 \mu\text{m}$ ). The experimental uncertainties of the phonon frequencies have been estimated to be of  $\pm 0.2 \text{ cm}^{-1}$ .

The size and shape of dots under study have been determined by means of AFM. Figure 1 presents an example of an image of InN islands lying on the surface of the GaN buffer layer, identified as “white” hexagons. By scanning different parts of this sample, the diameter variation was found to be

rather narrow ( $\pm 10\%$ ). From a higher magnification image (b) on a single island, we determined a diameter of  $0.5 \mu\text{m}$  and a height of  $0.18 \mu\text{m}$ ; the shape corresponds to a perfect hexagon in the film plane and to a truncated pyramid in the vertical direction. Samples obtained using different growth times have been investigated and the usual shape is characterized by the following features: the ratio of top surface diameter by base surface diameter ( $d$ ) is close to 0.5. In addition, the ratio between the height ( $h$ ) of the dots and  $d$  ranges from 0.07 for the small dots up to 0.4 for larger dots.

Among islands of different sizes investigated, we choose to show and discuss results obtained on the largest ones, where the spatial resolution of the micro-Raman probe allowed the detection of the heterogeneity in the strain profile across the island. To illustrate this finding, we present in Fig. 2 three examples of Raman spectra recorded at room temperature outside an isolated island (a), inside the island (c), and in an intermediate position (b), each position being identified in the optical image of the sample surface. InN dots appear clearly as hexagonal deposits with a low density ( $\sim 8 \times 10^6 \text{ cm}^{-2}$ ). The corresponding spectra have been acquired in a backscattering geometry along the (0001) direction. In Fig. 2(a), the two main peaks observed at  $570$  and  $735 \text{ cm}^{-1}$  are assigned to the long-wavelength  $E_2$  and  $A_1$  [longitudinal optical (LO)] symmetry phonons of GaN, respectively, in agreement with Raman selection rules imposed by the wurtzite structure. The natural response of the grating of the microspectrometer leads to a partially crossed polarization analysis which is responsible for the low intensity of the  $A_1(\text{LO})$  mode with respect to the  $E_2$  mode. Other peaks related to the InN material are also observed in Fig. 2(b) at  $491$  and  $589 \text{ cm}^{-1}$ , respectively, corresponding to the  $E_2$  and  $A_1(\text{LO})$  phonons of InN. These frequencies are slightly higher than their values in InN single crystal or in thin layers.<sup>16,24</sup> In Fig. 2(c), when the laser spot is located just upon the single island, the signature of the GaN phonons is no longer obtained, suggesting that the excitation light is strongly absorbed in InN due to its low electronic band gap. A new broadband appearing at  $440 \text{ cm}^{-1}$  is assigned to the activation of scattering by the  $A_1(\text{TO})$  phonon of InN. Moreover, the slope observed at  $200 \text{ cm}^{-1}$  (cutoff of the dielectric edge filters) could be related to the phonon density of states in the region of the low-frequency  $B_1$  mode of InN.<sup>16</sup> Defects, such as interface dislocations, reported by Feuillet *et al.*<sup>9</sup> in InN dots are believed to play a key role in the  $\mathbf{q}$  nonconserving process, and, consequently, in the activation of forbidden scattering. A careful analysis of these spectra revealed some changes in InN phonon frequencies. A plot of frequency as a function of position across the large dot is given in Fig. 3. Both the  $E_2$  and  $A_1(\text{LO})$  modes experience a blueshift (of  $+1$  and  $+2 \text{ cm}^{-1}$ , respectively) when measured in the facets of the dot with respect to its value in the dot center. All these data [in particular the homothetic shift of the  $E_2$  and  $A_1(\text{LO})$  phonon frequencies] can be accounted for by strain effects. Indeed, due to the large lattice mismatch and to the difference of expansion coefficients between InN and GaN, a compressive in-plane [i.e., perpendicular to the (0001) axis] strain is expected in the dots. Raman selection

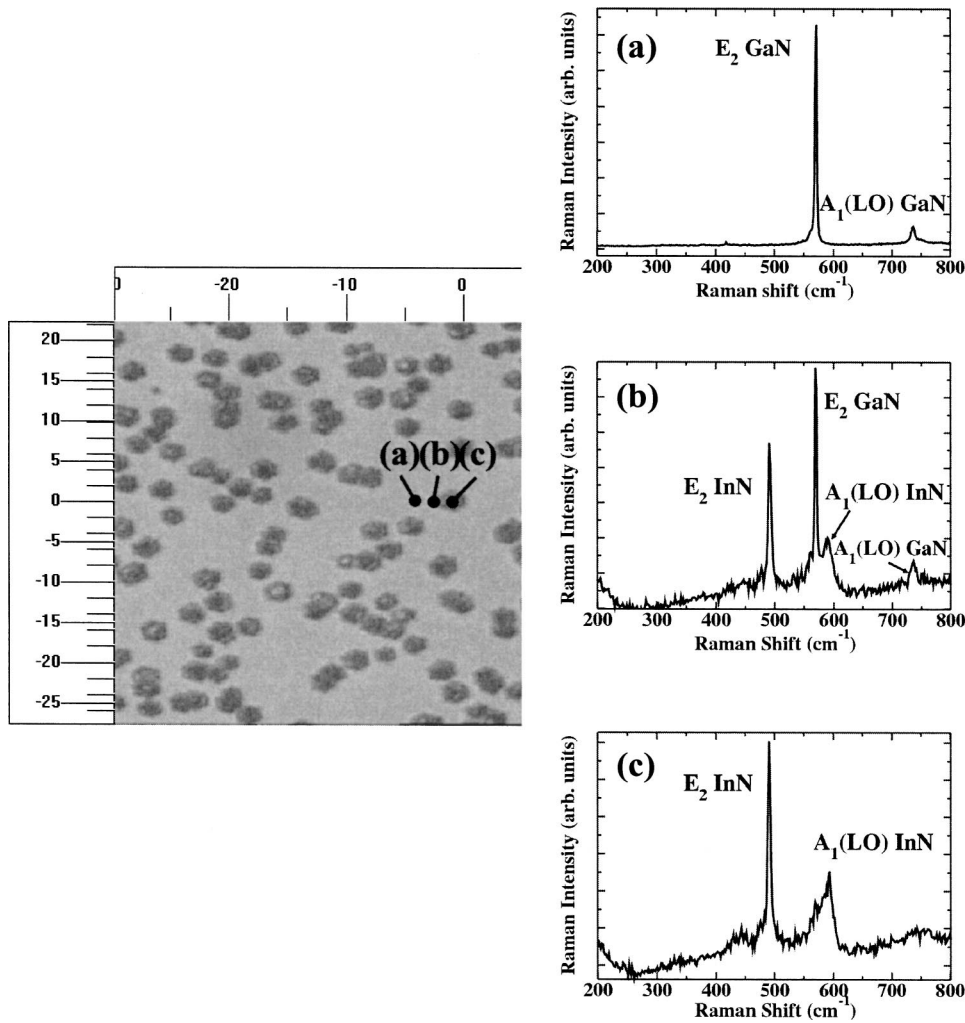


FIG. 2. Optical image (50 × 50 μm) of the sample surface exhibiting large InN islands (diameter of 2.4 μm). Example of Raman spectra recorded from outside the island (a), from the island center (c), and from an intermediate position (b).

rules attest that the hexagonal structure is maintained in the InN dots, consequently the frequency shift is given by

$$\Delta\omega = \omega - \omega_0 = 2a\varepsilon_{xx} + b\varepsilon_{zz},$$

where  $\omega_0$  represents the  $E_2$  phonon frequency in relaxed InN material,  $a$  and  $b$  are the appropriate phonon deformation potentials, and  $\varepsilon_{xx}$  and  $\varepsilon_{zz}$  represent the strains perpendicular and parallel to the  $z$  axis. Currently  $a$  and  $b$  are not available for InN, but these parameters were found to be negative and close to each other for GaN and AlN.<sup>26–28</sup> We will consider that the same holds for InN. In addition, under a compressive

biaxial stress (which is likely for the present dots), strains obey the inequality  $\varepsilon_{xx} < -\varepsilon_{zz} < 0$ . Therefore,  $\Delta\omega$  is expected to be positive, as found experimentally. Internal strains of the present InN island could be derived from the measured frequency shift of the  $E_2$  phonon of InN (+3 cm<sup>-1</sup>). If its deformation potentials would be close to those reported for GaN by Davydov *et al.*,<sup>27</sup> strain would be low but far from negligible ( $\varepsilon_{xx} \approx -0.38\%$ ). Consequently, the strain variation across the dot would be of +0.1%. These qualitative estimations present some significant discrepancies with the relationship between the  $E_2$  phonon frequency and the in-plane strain given by Kurimoto *et al.*<sup>15</sup> In this work, a tentative estimation of the strain has been proposed by considering the residual thermal strain, depending on the growth temperature and induced by the different thermal-expansion coefficient of sapphire and InN. According to this hypothesis, the  $E_2$  phonon would experience a blueshift of +3 cm<sup>-1</sup> for a strain variation ( $\Delta\varepsilon_{xx}$ ) of 0.05%, which yields a surprising slope  $\Delta\omega_{E_2}/\Delta\varepsilon_{xx}$  eight times higher than its counterpart for GaN. We believe that the results reported in Ref. 15 would need to be checked by combining x-ray and Raman analysis in InN layers.

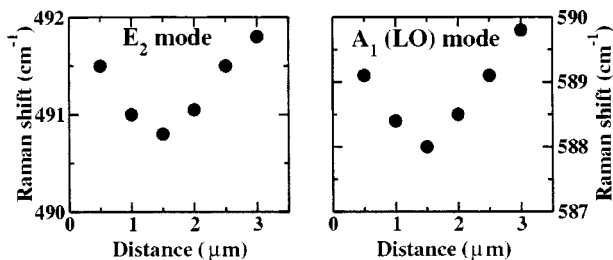


FIG. 3. Plot of the frequency of  $E_2$  and  $A_1(\text{LO})$  phonons of InN vs the distance across the island imaged in Fig. 2. “0” value corresponds to the island border.

In order to get a further interpretation of the strain variation inside the dot, we plot in Fig. 4 the frequency of the  $E_2$

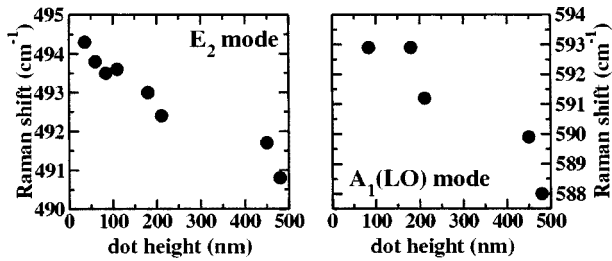


FIG. 4. Plot of the frequency of  $E_2$  and  $A_1(\text{LO})$  phonons of InN vs the dot height ( $h$ ).

and  $A_1(\text{LO})$  modes versus island height  $h$ , derived from Raman measurements on single dots of different size (not shown). A detailed analysis of these data makes clear that the dot aspect ratio (i.e.,  $h/d$ ) is not a key parameter in determining the internal strain but rather  $h$ . Indeed, the plot of the  $E_2$  mode frequency versus the  $h/d$  ratio (not shown) reveals a collection of randomly distributed points for which any correlation is impossible. From the plot proposed in Fig. 4, strain (derived from the Raman mode frequencies) appears to vary linearly as a function of the height of the dot. The linear dependence of the  $E_2$  mode frequency and  $h$  is not in question, however this is not so obvious for the  $A_1(\text{LO})$  mode, which will be discussed later. From these results, the density of threading dislocations is believed to increase when  $h$  is increasing, leading to a higher degree of relaxation of strain for increasing distances to the interface. The in-plane mismatch of 11% between InN and GaN is mainly relaxed by plastic relaxation starting at a few nanometers from the interface. Such an issue would also be a possible explanation for the strain heterogeneity found in the larger dots. The micro-Raman probe is sensitive to an increasing local strain since island facets are regions with a thickness gradient. Similar trends have been observed by Kegel *et al.*<sup>29</sup> in the mismatched ( $\sim 7\%$ ) InAs/GaAs system, from fully strained at the bottom of InAs dots to completely relaxed at the top surface. From the plot of Fig. 4, a  $+3.5 \text{ cm}^{-1}$  shift is observed between the larger and the smaller islands. We deduce a strain of approximately  $-0.6\%$  in small islands. Our estimation is in agreement with results obtained by synchrotron x-ray scattering in InN films grown directly on sapphire.<sup>30</sup>

In both Figs. 3 and 4, the  $A_1(\text{LO})$  phonon exhibits a frequency shift approximately two times larger than the  $E_2$  mode, which renders the  $\delta\omega[A_1(\text{LO})]/\delta\omega[E_2]$  ratio stronger than its usual value previously reported in GaN.<sup>26</sup> The ratio obtained in the present study is probably due to angular dispersion of the polar optical phonons, which is related to the anisotropy of the wurtzite structure. Light entering through the facets of the dots confers to the phonon a propagation direction tilted by an internal angle  $\theta$  with respect to the (0001) axis. In that case, modes with dominant transverse optical (TO) and LO characters, the so-called quasi-TO and quasi-LO (QLO) modes, exhibit mixed ( $A_1, E_1$ ) symmetry. Their frequencies versus  $\theta$  evolve continuously between the values of  $\omega[A_1(\text{LO})]$  and  $\omega[E_1(\text{LO})]$ ,<sup>31</sup>

$$\omega_{\text{QLO}}^2 = \omega_{A_1(\text{LO})}^2 \cos^2 \theta + \omega_{E_1(\text{LO})}^2 \sin^2 \theta.$$

Finally, we performed some complementary measurements on InN islands which have been capped by covering the surface with a  $0.7\text{-}\mu\text{m}$ -thick GaN layer deposited at a rather low temperature to prevent the thermal degradation of the underlying InN islands. In that case, we measured a weakly increased strain state in large dots ( $1.5 \mu\text{m}$  in diameter) giving a new confirmation of the previous conclusion about the nature of the strain relaxation at the InN/GaN interface. A Raman shift of  $+2.3 \text{ cm}^{-1}$  was measured for the  $E_2$  phonon after capping, which is as high as the difference measured between relaxed InN and the uncapped dots grown on GaN. In comparison with GaN dots grown on AlN, the deduced strain variation ( $-0.3\%$ ) is quite low, showing again the major role of plastic relaxation near the new InN/GaN interface, which prevents measuring any retroactive effects on InN island internal strain.

In summary, we determined by AFM the morphology of single InN dots grown on GaN, and we correlated it to the estimated magnitude of the in-plane strain. Dots exhibit a weak compressive strain which slightly increases in smaller islands. Plastic strain relaxation by formation of a high density of dislocations is determined to be responsible for this low strain. Consequently, capping of the dots was found to lead to only a very slight increase of their internal strain. In the future, a quantitative determination of the strain state in InN dots will require a combination of x-ray and Raman scattering analysis on 2D thin InN layers.

<sup>1</sup>J. Gleize, J. Frandon, F. Demangeot, M. A. Renucci, C. Adelman, B. Daudin, G. Feuillet, B. Damilano, N. Grandjean, and J. Massies, *Appl. Phys. Lett.* **77**, 2174 (2000).

<sup>2</sup>M. Kuball, J. Gleize, S. Tanaka, and Y. Aoyagi, *Appl. Phys. Lett.* **78**, 987 (2001).

<sup>3</sup>F. Bechstedt and J. Furthmüller, *J. Cryst. Growth* **246**, 315 (2002).

<sup>4</sup>V. Yu. Davydov, A. A. Lochikhin, R. P. Seisyan, V. V. Emtsev, S. V. Ivanov, F. Bechstedt, J. Furthmüller, H. Harima, A. V. Mudryi, J. Aderhold, O. Semchinova, and J. Graul, *Phys. Status Solidi B* **229**, R1 (2002).

<sup>5</sup>J. Wu, W. Walukiewicz, K. M. Yu, J. W. Ager, E. E. Haller, H. Lu, and W. J. Schaff, *Appl. Phys. Lett.* **80**, 4741 (2002).

<sup>6</sup>V. Yu. Davydov, A. A. Lochikhin, V. V. Emtsev, S. V. Ivanov, V. V. Vekshin, F. Bechstedt, J. Furthmüller, H. Harima, A. V. Mudryi, A. Hashimoto, J. Aderhold, J. Graul, and E. E. Haller, *Phys. Status Solidi B* **230**, R4 (2002).

<sup>7</sup>T. Matsuoka, H. Okamoto, M. Nakao, H. Harima, and E. Kurimoto, *Appl. Phys. Lett.* **81**, 1246 (2002).

<sup>8</sup>Z. Yuan, B. E. Kardynal, R. M. Stevenson, A. J. Shields, C. Lobo, K. Cooper, N. S. Beattie, D. A. Ritchie, and M. Pepper, *Science* **295**, 102 (2002).

<sup>9</sup>G. Feuillet, B. Daudin, F. Widmann, J. L. Rouvière, and M. Arlery, *J. Cryst. Growth* **189**, 142 (1998).

<sup>10</sup>O. Briot, B. Maleyre, S. Ruffenach, *Appl. Phys. Lett.* (to be published).

- <sup>11</sup>G. Pozina, J. P. Bergman, B. Monemar, V. V. Mamutin, T. V. Shibina, V. A. Vekshin, A. A. Toropov, S. V. Ivanov, M. Karrlsteent, and M. Willander, *Phys. Status Solidi B* **216**, 445 (1999).
- <sup>12</sup>C. H. Liang, L. C. Chen, J. S. Hwang, K. H. Chen, Y. T. Hung, and Y. F. Chen, *Appl. Phys. Lett.* **81**, 22 (2002).
- <sup>13</sup>H.-J. Kwon, Y.-H. Lee, O. Miki, H. Yamano, and A. Yoshida, *Appl. Phys. Lett.* **69**, 937 (1996).
- <sup>14</sup>M.-C. Lee, H.-C. Lin, Y.-C. Pan, C.-K. Shu, J. Ou, W.-H. Chen, and W.-K. Chen, *Appl. Phys. Lett.* **73**, 2606 (1998).
- <sup>15</sup>E. Kurimoto, H. Harima, A. Hashimoto, and A. Yamamoto, *Phys. Status Solidi B* **228**, 1 (2001).
- <sup>16</sup>V. Yu Davydov, V. V. Emtsev, I. N. Goncharuk, A. N. Smirnov, V. D. Petrikov, V. V. Mamutin, V. A. Vekshin, and S. V. Ivanov, *Appl. Phys. Lett.* **75**, 3297 (1999).
- <sup>17</sup>A. Tabata, E. Silveira, J. R. Leite, R. Trentin, L. M. R. Scolfaro, V. Lemos, T. Frey, D. J. As, D. Schikora, and K. Lischka, *Phys. Status Solidi B* **216**, 769 (1999).
- <sup>18</sup>G. Kaczmarczyk, A. Kaschner, S. Reich, A. Hoffmann, C. Thomssen, D. J. As, A. P. Lima, D. Schikora, K. Lischka, R. Averbeck, and H. Riechert, *Appl. Phys. Lett.* **76**, 2122 (2000).
- <sup>19</sup>F. Agulló-Rueda, E. E. Mendez, B. Bojarczuk, and S. Guha, *Solid State Commun.* **115**, 19 (2000).
- <sup>20</sup>A. Kasic, M. Schubert, Y. Saito, Y. Nanishi, and G. Wagner, *Phys. Rev. B* **65**, 115206 (2002).
- <sup>21</sup>K. Xu and A. Yoshikawa, *Appl. Phys. Lett.* **83**, 251 (2003).
- <sup>22</sup>T. Inushima, T. Shiraishi, and V. Yu Davydov, *Solid State Commun.* **110**, 491 (1999).
- <sup>23</sup>Z. G. Qian, W. Z. Shen, H. Ogawa, and Q. X. Guo, *J. Appl. Phys.* **93**, 2643 (2003).
- <sup>24</sup>J. S. Dyck, K. Kim, S. Limpijumnong, W. R. L. Lambrecht, K. Kash, and J. C. Angus, *Solid State Commun.* **114**, 355 (2000).
- <sup>25</sup>C. Bungaro, K. Rapcewicz, and J. Bernholc, *Phys. Rev. B* **61**, 6720 (2000).
- <sup>26</sup>F. Demangeot, J. Frandon, M. A. Renucci, O. Briot, B. Gil, and R. L. Aulombard, *Solid State Commun.* **100**, 207 (1996).
- <sup>27</sup>V. Yu Davydov, N. S. Averkiev, I. N. Goncharuk, D. K. Nelson, I. P. Nikitina, A. S. Plkovnikov, A. N. Smirnov, M. A. Jacobson, and O. K. Semchinova, *J. Appl. Phys.* **82**, 5097 (1997).
- <sup>28</sup>J. Gleize, J. Frandon, M. A. Renucci, E. Bellet-Amalric, and B. Daudin, *J. Appl. Phys.* **93**, 2065 (2003).
- <sup>29</sup>I. Kegel, T. H. Metzger, P. Fratzl, J. Peisl, A. Lorke, J. M. Garcia, and P. M. Petroff, *Europhys. Lett.* **45**, 222 (1999).
- <sup>30</sup>I. J. Lee, J. W. Kim, Y.-H. Hwang, and H.-K. Kim, *J. Appl. Phys.* **92**, 5814 (2002).
- <sup>31</sup>R. Loudon, *Proc. R. Soc. London, Ser. A* **275**, 218 (1963).